

Tripterygium wilfordii derivative LLDT-8 targets CD2 in the treatment of rheumatoid arthritis

YUAN LI, WUFANG QI, LEI YAN, MENGMENG WANG and LINRU ZHAO

Department of Rheumatology and Clinical Immunology, Tianjin First Central Hospital, Tianjin 300192, P.R. China

Received December 7, 2020; Accepted March 24, 2021

DOI: 10.3892/br.2021.1457

Abstract. Rheumatoid arthritis (RA), a chronic inflammatory synovitis systemic disease, can lead to joint deformities, loss of function and even death. The pathogenesis of RA may be related to genetics, infection and/or sex hormones; however, detailed accounts of the molecular mechanisms underlying its pathogenesis are lacking. In the present study, the synovial tissues of patients with RA and healthy individuals were analyzed to identify the pathogenic signaling pathways and key candidate genes involved in RA. Gene Ontology (GO), pathway enrichment and protein-protein interaction analysis were further used to identify the differentially expressed genes (DEGs) and their potential roles in RA. Molecular docking was used to screen the potential candidate drugs for management of RA. Small interfering RNA was used for knockdown of the CD2 protein. A Cell Counting Kit-8 assay was used to detect the proliferation of cells. Changes in the levels of inflammatory cytokines were detected using ELISA. A total of 279 DEGs were identified in RA; amongst these genes, 166 and 113 were upregulated and downregulated, respectively. GO analysis revealed that the upregulated DEGs were primarily enriched in the activation of the immune and adaptive immune responses, as well as the inflammatory response. The T-cell surface antigen CD2 (CD2) was identified as the most important hub gene by selecting the most important module from the protein-protein interaction network. Knockout of CD2 reduced the damaging effects of TNF- α on synovial cells. Through in situ screening using computer-aided drug design, the triptolide derivative (5R)-5-hydroxytriptolide (LLDT-8) was determined to have the highest docking score based on the CD2 protein structure. Cell experiments showed that LLDT-8 could inhibit the expression of CD2. Cell proliferation and inflammatory cytokine assays confirmed that CD2 was the direct target of

LLDT-8. Together, the results of the present study determined factors involved in the pathogenesis of RA and the important role of CD2 in this process by analyzing the DEGs in the RA process. LLDT-8 inhibited CD2 and may thus be used to treat RA. These candidate genes and signaling pathways may serve as potential targets for the clinical treatment of RA.

Introduction

Rheumatoid arthritis (RA), a chronic inflammatory disease, is primarily characterized by the symmetrical distribution of invasive joint inflammation of the hands, feet, blood vessels or related connective tissues (1,2). RA occurs in patients of all ages, and is a serious health burden as well as an economic and social burden (3).

In general, genetic and environmental factors are the primary factors attributed to RA, and immune disorders are considered to be the primary pathogenic factors (4-6). Exogenous or endogenous antigens activate T cells, which release inflammatory cytokines. T cells activate B cells to produce a series of antibodies that induce immune disorders, which damage various types of tissues (7). However, the mechanism by which the immune disorder is induced, and how the disease further worsens during the process of RA is not well explained and requires in-depth research. The efficacy of several drugs used to alleviate the pain of patients with RA is limited, and the side effects are evident (8). Therefore, the development of novel and effective drugs for RA treatment is required.

Expression profiling is increasingly used to analyze disease-related genes or signaling pathways to determine the pathogenesis of numerous diseases (9,10). T-cell surface antigen CD2 (CD2) can interact with lymphocyte function associated antigens CD58 and CD48/BCM1 to mediate adhesion between T cells and other cell types. CD2 is also involved in T cell induction, and the cytoplasmic domain is involved in signal transduction. It also serves an important role in the inflammatory response. LLDT-8 is a novel RA drug. Pharmacological analysis has shown that LLDT-8 is a new diterpene compound of *Tripterygium wilfordii* with low toxicity and high efficiency and strong immunosuppressive activity *in vitro* and *in vivo*. In addition, it has been reported that LLDT-8 inhibits osteoclastogenesis via regulation of the RANKL/RANK/OPG signaling pathway (11). LLDT-8 protects against cerebral ischemia/reperfusion injury by

Correspondence to: Dr Yuan Li or Dr Linru Zhao, Department of Rheumatology and Clinical Immunology, Tianjin First Central Hospital, 24 Fukang Road, Tianjin 300192, P.R. China
E-mail: etigerli@126.com
E-mail: 13821005277@163.com

Key words: rheumatoid arthritis, bioinformatics, T-cell surface antigen CD2, LLDT-8, molecular screening

suppressing post-stroke inflammation (12). LLDT-8 can protect against bleomycin-induced lung fibrosis in mice (13). However, the effect of LLDT-8 as a treatment for RA remains to be further studied.

In the present study, differentially expressed genes (DEGs) related to RA were screened through bioinformatics analysis of the expression profile data of clinical RA and normal tissue samples. A key node gene regulating RA was further selected using topological analysis. Finally, traditional Chinese medicine (TCM) libraries were molecularly screened on the basis of the key node gene to identify potential therapeutic drugs.

Materials and methods

Microarray data information and data preprocessing. GSE55235 and GSE84074 microarray data were downloaded from the GEO database (ncbi.nlm.nih.gov/geo/) (14). The GSE55235 chip data was based on GPL96, [hg-u133a] Affymetrix Human Genome U133A Array (15). The Affymetrix, Calif. GSE84074 chip was based on the GPL19640, agilent-062918 Human lncRNA array version 4.0 (Probe name version) microarray data in Bioconductor (version 1.46.1; bioconductor.org/) (16). The preprocessing stage included background correction, normalization and expression calculation. The Bioconductor Annotation data package was used to convert the chip data probe into gene symbols. If multiple probes were mapped to a gene symbol, the average was set for the final expression value of the gene. The DEGs of each group were analyzed using the limma package (17). The DEGs were analyzed using the volcano map script in the R studio (version 1.2.5042) (18,19). $P < 0.05$ and $\log_2(\text{fold change}) \text{FCI} > 2$ were used as the cutoff criteria. The Heatmap package was used for hierarchical clustering analysis and visualization of DEGs (20).

GO and pathway enrichment analysis. The Clue-GO plugin in Cytoscape (21) was used to analyze the functions and pathways of the DEGs. $P < 0.05$ was used as the cutoff criteria. Enrichment analysis was performed and visualized using ClueGO and CluePedia with $P < 0.05$ as the cutoff criterion (22-24). The function and pathway enrichment analysis of DEGs following LLDT-8 processing was performed using the clusterProfiler package (25).

Cell culture. Synoviocytes were purchased from Shanghai Institute of Biochemistry and Cell Biology. Synovial cells were grown in DMEM supplemented with 10% FBS (Gibco; Thermo Fisher Scientific, Inc.) in a humidified incubator at 37°C with 5% CO₂.

Cell transfection. Cells in the logarithmic growth phase were used for transfection. A total of 4×10^5 cells/well were plated in a 6-well plate and 2 ml supplemented media without antibiotics was added. Transfection was performed when the confluence of cells reached 70%. For transfection, the negative control small interfering (si)RNA was used, and for the experimental group si-CD2 was added. Transfections were performed using Lipofectamine™ 2000 (Thermo Fisher Scientific, Inc.). The final siRNA concentration used was 40 nmol/l. The sequences of the siRNAs were: si-NC, 5'-UUCUCCGAACGUGUCACG

UTT-3' and 5'-ACGUGACACGUUCGGAGAATT-3'; and for si-CD2, 5'-CCAAAGGUGCAGUCUCCAATT-3' and 5'-UUGGAGACUGCACCUUUGGTT-3'. The siRNAs were purchased from Santa Cruz Biotechnology, Inc. Follow-up experiments were performed 48 h after transfection.

Cell proliferation assay. Cell proliferation was detected using a Cell Counting Kit-8 (CCK-8) assay. A total of 1×10^3 cells in 200 μl were added per well to a 96-well plate. Following the different treatments, 10 μl CCK-8 solution (Dojindo Molecular Technologies, Inc.) was added to each well, and the plate was further incubated for 2 h in a 5% CO₂ incubator. The absorbance of cells was measured using a microplate reader at 450 nm. All experiments were repeated 3 times.

Reverse transcription-quantitative (RT-q)PCR. Cells were seeded in 6-well plates containing 2 ml complete medium at a density of 1×10^6 . The 6-well plates were incubated at 37°C, 5% CO₂ and 100% humidity for 24 h. TNF- α (10 ng/ml; cat. no. 14-8329-62; Thermo Fisher Scientific, Inc.) or IL-1 β (10 mg/l; cat. no. SRP3083; Sigma-Aldrich; Merck KGaA) was added to stimulate the cells for 24 h. Total RNA was extracted using TRIzol® (cat. no. 15596026; Thermo Fisher Scientific, Inc.). Isolated RNA was reverse transcribed into cDNA using a reverse transcription kit according to the manufacturer's protocol (cat. no. RR036A; Takara Bio, Inc.). The sequences of the primers were: CD2 forward, 5'-CCCATGATTCCTTCATATTTGCA-3' and reverse, 5'-GGTCCTTCTCCAGCCTAGT-3'; IL-6 forward, 5'-CCACTCACCTCTTCAGAACG-3' and reverse, 5'-CATCTTGGAAAGGTTTCAGGTTG-3'; LDH forward, 5'-GTTGGAAGCTGGTGCCGTAG-3' and reverse, 5'-GAAAAGACTGCCATGCTGAAG-3'; IL-1 β forward, 5'-CCTGTCTGCGTGTTGAAAGA-3' and reverse, 5'-GGGAACTGGGCAGACTCAAA-3'; and β -actin forward, 5'-GATCTTGATCTTCATGGTGCTAG-3' and reverse, 5'-TTGTAACCACCTGGGACGATATGG-3'. β -actin was used as the internal reference. For qPCR, 10 μl cDNA was used per sample, and the thermocycling conditions were: 95°C for 5 min; followed by 40 cycles of 95°C for 10 sec and 60°C for 30 sec. The 2^{- $\Delta\Delta\text{C}_q$} method was used for relative quantitative analysis (26).

Detection of cellular inflammatory factors. LDH and IL-6 ELISA kits (Beijing Solarbio Science & Technology Co., Ltd.) were used to detect the levels of inflammatory factors in cells following the different treatments, according to the manufacturer's protocol.

Protein-protein interaction (PPI) networks. The CentiScape plugin (27) was used to calculate the node degree, and the molecular complex detection (MCODE) plugin (28) was employed to find clusters in the entire PPI network. Nodal proteins may have important physiological regulatory functions and may be key candidate genes. The genes in the most significant modules were extracted for functional enrichment analysis. $P < 0.05$ was set as the cutoff value.

Integration of the PPI network. The online database STRING (string-db.org) was used to construct the PPI network of DEGs (29). Cytoscape was used to construct the protein interaction network and analyze the interactive relationship of the

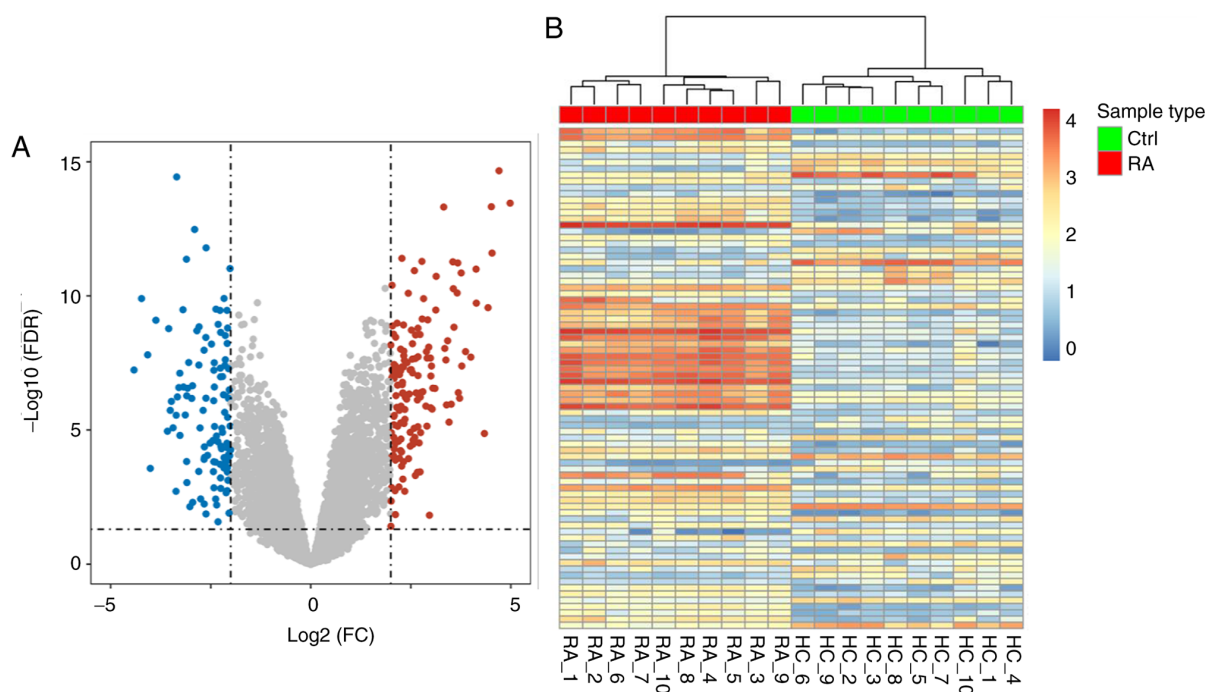


Figure 1. Identification of differentially expressed genes in RA. (A) Volcano plots of the DEGs between normal and RA joint synovial tissue samples. Red and green dots indicate the upregulated and downregulated genes, respectively. The black dots correspond to gene expression with $\log_2\text{FC} < 2$. The Y-axis represents the FDR, and the X axis denotes the value of $\log_2\text{FC}$. (B) Heatmap of DEGs between RA and normal synovial tissues based on the expression profiles.

candidate DEGs encoding proteins in RA. Hub genes were determined on the basis of the degree results.

Molecular docking. The protein structure of CD2 was downloaded from the PDB database (rcsb.org; PDB ID, 1HNF) (30). Schrödinger (Maestro-2015-2) software was used to optimize the structure of the protein, which included assigning bond sequences, hydrogenating atoms, and removing eclipsed conformations. Finally, the energy of CD2 was minimized. The Schrödinger LigPred module was used to optimize the energy of the small molecule structure (31). First, 651 Chinese medicine molecules with the highest CD2 docking scores were screened using high throughput virtual (HTV) screening. The standard precision (SP) screen was selected from 34 Chinese medicine molecules. Finally, three candidate Chinese medicine molecules (extra precision screen) were obtained via precise docking. PyMOL (version 2.3) (32) was used to visualize the structures of triptolide derivative (5R)-5-hydroxytriptolide (LLDT-8) and CD2.

Gene set enrichment analysis (GSEA). Genes that may serve a key role in RA were determined through the statistical calculation on the basis of GSEA (version 3.0) (33), which was used to compare the genes to be analyzed with those that were pre-divided into gene sets. The input file in the GCT/CLS format was created in accordance with the format requirements of the software. The CLS file was the grouping description file of the expression matrix of sequencing data, and the GCT file was the gene expression matrix files in sequencing. For data analysis, the parameters were set as: Number of permutations, 1,000; Collapse dataset to gene symbols, true; Permutation type, gene_set; Max size, exclude larger sets, 500; Min size, exclude smaller sets: 15.

Statistical analysis. SPSS version 20.0 (IBM, Corp.) was used for analysis, and measurement data are expressed as the mean \pm standard deviation. Comparisons between two groups were performed using a Student's t-test, and comparisons between multiple groups were performed using a one-way ANOVA followed by a post-hoc Tukey's test. $P < 0.05$ was considered to indicate a statistically significant difference.

Results

Identification of DEGs in RA, and GSEA of the DEGs. Data were downloaded from NCBI-GEO, a public functional genomics database that receives data from different microarray platforms, and the gene expression profiles of RA and normal synovial tissues were obtained from the GSE55235 dataset (15). The data included synovial tissues from 10 patients with RA and 10 individuals with healthy joints. $P < 0.05$ and $\log_2(\text{fold change}) \text{FC} > 2$ were used as the cutoff criteria. A total of 279 DEGs (166 upregulated and 113 downregulated genes) were extracted from the expression profile dataset (Fig. 1A). The DEGs are shown as a heatmap based on the $\log_2\text{FC}$ value in Fig. 1B. According to the results, the DEGs identified could be used to distinguish RA from the normal group and could be used for subsequent biological analysis. The GSEA software package was used to analyze the different biological processes of synovial tissues in patients with RA and healthy individuals, and the truncated value was $P < 0.05$. GSEA is a computational method used to determine whether a predefined set of genes can show significant consistent differences in two biological states. In the GO analysis, the upregulated functions associated with the significantly enriched genes included the activation of immune and adaptive immune responses. The connective

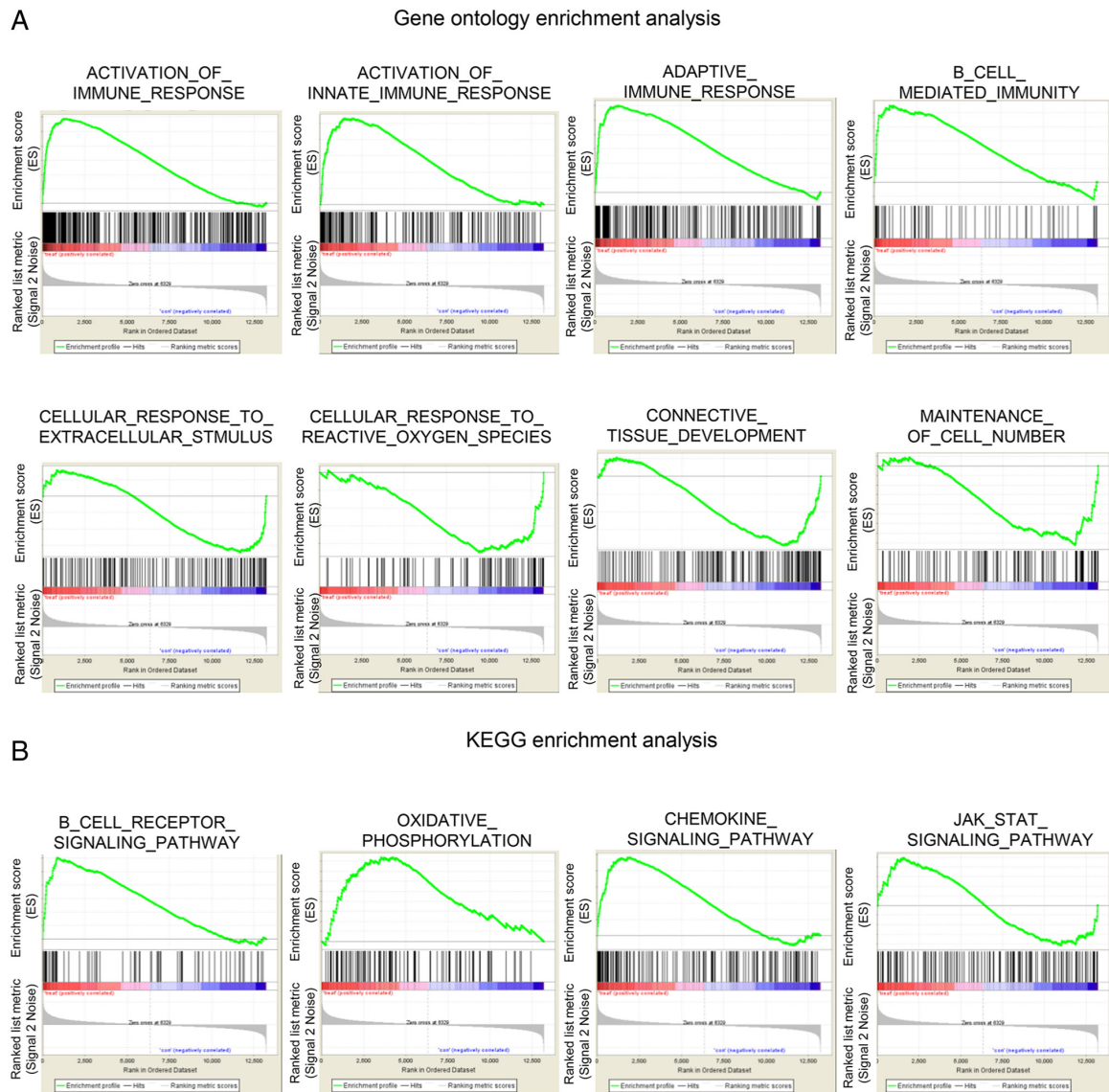


Figure 2. GSEA analysis of DEGs in RA. (A) GO function enrichment analysis of DEGs. (B) Immune-related pathways were activated during RA based on KEGG enrichment analysis. GO, Gene Ontology; DEG, differentially expressed gene; KEGG, Kyoto Encyclopedia of Genes and Genomes; FDR, false discovery rate; FC, fold change; Ctrl, control; RA, rheumatoid arthritis.

tissue development, cell number maintenance, and cellular response to extracellular stimulus function decreased (Fig. 2A). KEGG enrichment analysis showed that the B cell receptor, chemokine, the JAK-STAT signaling pathways and oxidative phosphorylation were activated in RA lesions (Fig. 2B). Identification of significantly rich functions and pathways may assist in further studying the role of DEGs in RA.

PPI network analysis of DEGs in RA. The study of protein interaction networks assist in deepening our understanding of cell structure and function from a systematic perspective and provide a theoretical basis for the discovery of novel drug targets and drug design. Using bioinformatics methods to study protein interaction network shows great advantages, including protein interaction network mapping and display, network topology analysis, network structure module research and network comparison. Based on the obtained DEGs, the interaction network of DEGs was further analyzed. The STRING database was used to calculate the PPI network (Fig. S1). As

observed from the results, the PPI network can be divided into five major interaction subset networks.

The key nodes in the PPI network were analyzed using Cytoscape plugins, to further analyze the hub genes in RA and determine the association of the protein interactions. The results showed that the interactive network had 41 nodes, 135 edges and a MCODE score of 6.750 (Fig. 3A). The degree of each node gene was further calculated, and CD2 had the highest topological connectivity (Fig. 3B). Furthermore, the Clue-GO plugin in Cytoscape software was used to enrich and annotate the key PPI module genes. Results showed that the key module genes were enriched primarily in response to corticosterone, antigen processing, and presentation of peptide or polysaccharide antigen via MHC class II, lymphocyte co-stimulation, interferon- γ -mediated signaling pathway, T cell co-stimulation and the T cell receptor signaling pathway (Fig. 3C).

CD2 is a key protein involved in the development of RA. According to the results of bioinformatics analysis, CD2 was

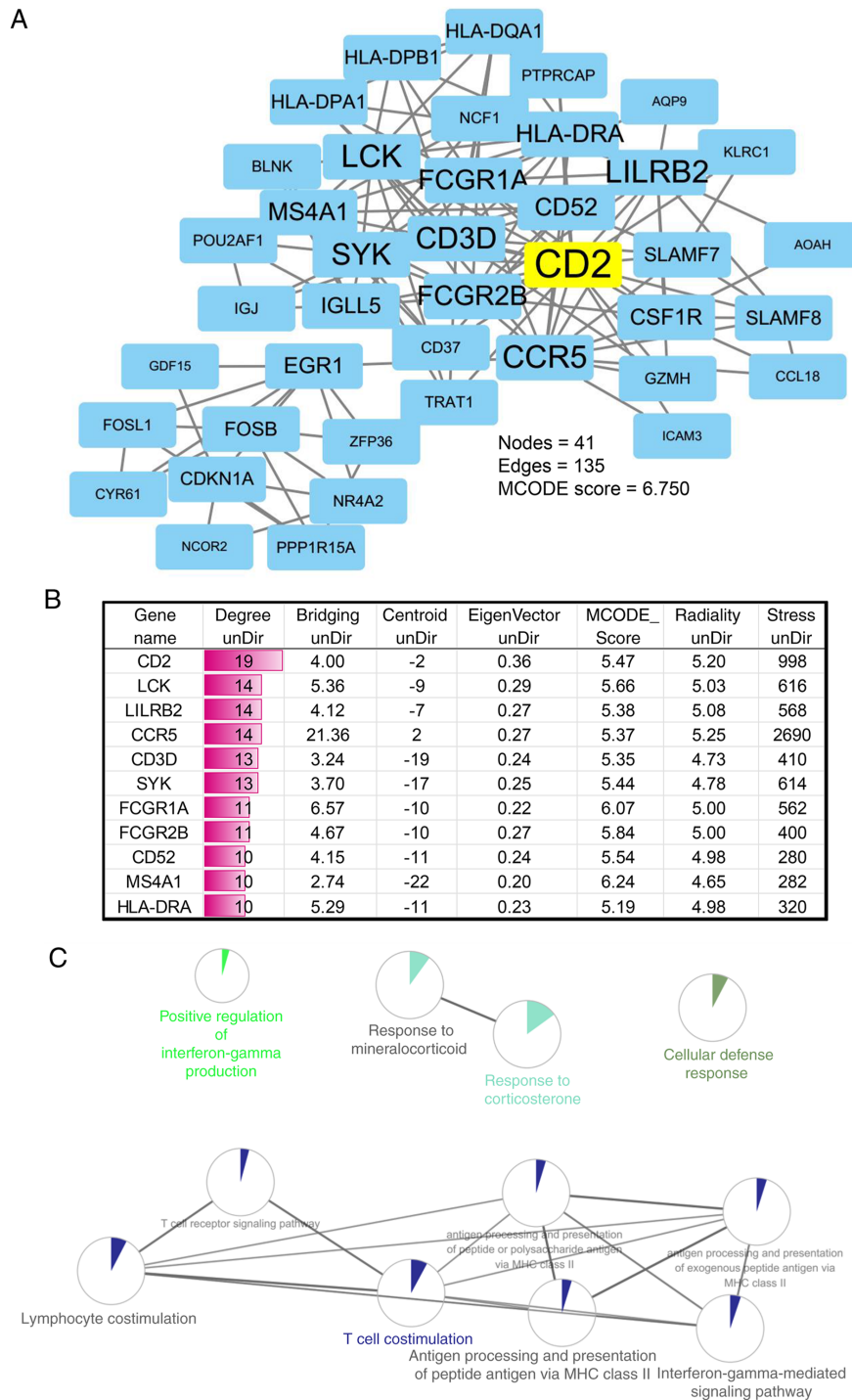


Figure 3. Identification of key genes in RA. (A) CD2 had the highest topological connectivity in the PPI network in RA. (B) Top 11 genes with high topological connectivity in the PPI network of RA associated genes. (C) PPI key module genes were widely involved in immune-related functions based on Clue-GO. GO, Gene Ontology; RA, rheumatoid arthritis; CD2, T-cell surface antigen CD2; PPI, protein-protein interaction.

determined to be a key protein involved in the development of RA. In order to verify the role of CD2 in RA, IL-1 and TNF- α were used to induce synovial cells for establishment of an *in vitro* RA cell model. The experimental results showed that IL-1 and TNF- α could induce the upregulation of CD2, consistent with the results of the bioinformatics analysis (Fig. 4A). Next, siRNAs were used to knockdown the expression of CD2. The experimental results show that the siRNAs effectively reduced the expression of CD2 (Fig. 4B). The results of cell proliferation experiments showed that

compared with the control group, CD2 knockdown reduced the inhibitory effect of TNF- α on proliferation in synovial cells (Fig. 4C). Furthermore, changes in the levels of cellular inflammatory factors were assessed. The results showed that compared with the control group, TNF- α stimulation increased the levels of inflammatory factors, whereas knockdown of CD2 reduced the effects of TNF- α (Fig. 4D-F).

Screening of TCMs that may inhibit key genes based on the structure of CD2. By analyzing the PPI network, CD2 was

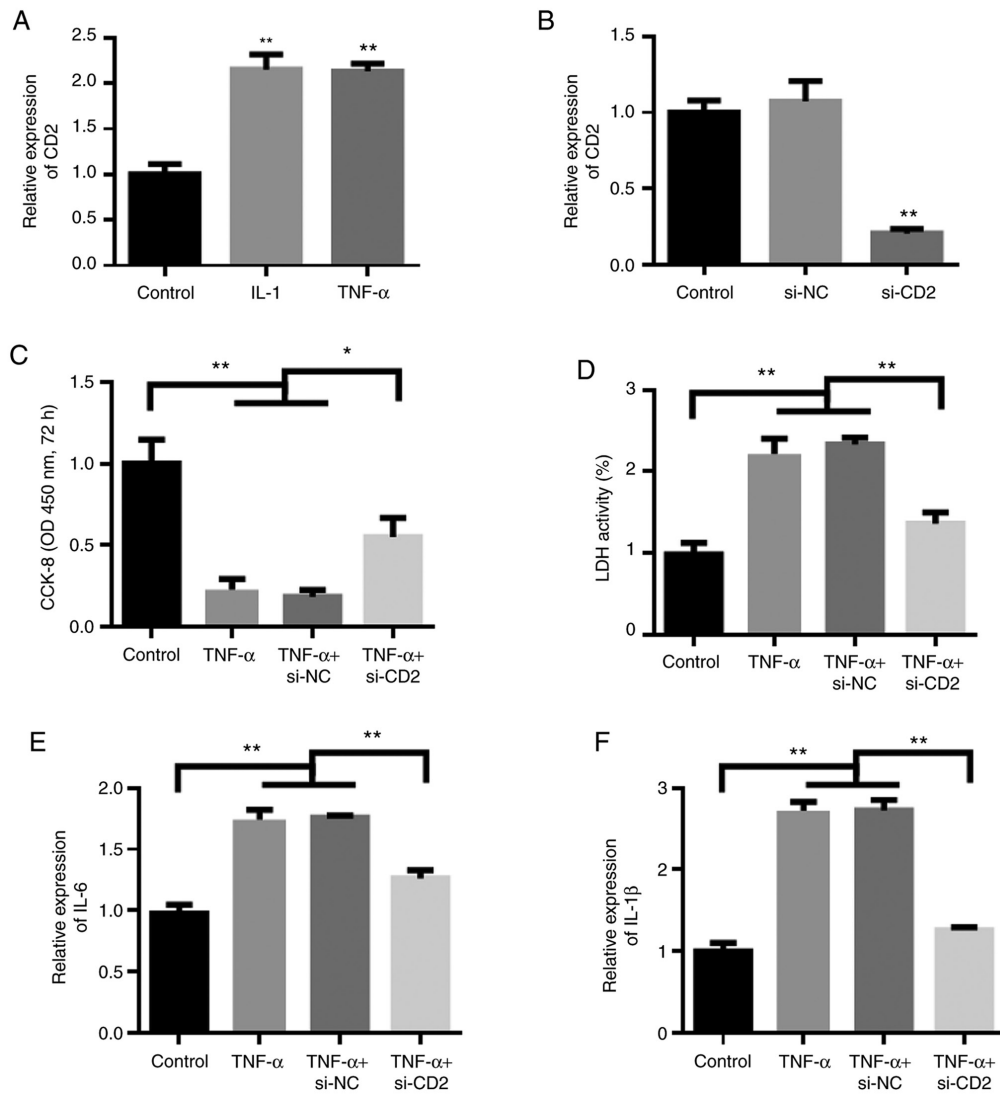


Figure 4. CD2 serves an important role in the occurrence and development of RA. (A) CD2 expression was detected following IL-1 and TNF- α stimulation of synovial cells. (B) siRNA knockdown efficiency was confirmed. (C) Cell proliferation ability was detected following the different treatments. (D) The levels of the cell inflammatory factor LDH were detected following different treatments. (E) Cytokine IL-6 levels were detected following the different treatments. (F) Cytokine IL-1 β levels were detected following different treatments. siRNA, small interfering RNA; CD2, T-cell surface antigen CD2; NC, negative control. * $P < 0.05$, ** $P < 0.01$.

found to be a key node gene that serves an important role in the pathogenesis of RA. CD2 was significantly upregulated in RA ($\log_{2}FC = 2.731$) and therefore was chosen as the basis for the selection of candidate compounds. A set of molecular screening strategies for TCM was designed on the basis of high-throughput virtual screening method. The schematic diagram of the screening process is shown in Fig. 5A. First, 651 Chinese medicine molecules with the highest CD2 docking scores were screened using a HTV screening. The SP screen was selected from 34 Chinese medicine molecules. Finally, three candidate Chinese medicine molecules (extra precision screen) were obtained via precise docking. Amongst these molecules, LLDT-8 and CD2 were found to have the highest docking score and the best binding mode (Fig. 5B). The binding between LLDT-8 and the target protein CD2 is shown in Fig. 5C. The key amino acid residues (Gln-15, Leu-13 and Arg-105) interacted with LLDT-8 to form a hydrogen bond interaction. The 3D conformation of LLDT-8 interacting with CD2 was used to further clarify their interaction. LLDT-8 may inhibit the function of CD2 by inhibiting its biological activity

center, and this inhibition may be beneficial for the management of RA.

LLDT-8 may exert its beneficial effects on RA through regulation of immunity and suppression of key pathways. A total of 324 DEGs were identified following pretreatment and batch elimination of DEGs in the GSE84074 dataset using the limma software package (16). Amongst these genes, 139 upregulated and 311 downregulated genes were identified in the LLDT-8 treatment group compared with the control group (Fig. 6A). DEGs are shown in the volcano plot, and the first 100 DEGs shown based on the value of $|\log_{2}FC|$ are also illustrated in the heatmap (Fig. 6B).

The function and pathway enrichment analysis of DEGs after LLDT-8 processing was performed using the clusterProfiler package (25). DEGs were divided into three functional groups, namely, biological process, molecular function and cellular component (Figs. 6C-D and 7A). LLDT-8 primarily inhibited the cellular response to IL-1, the positive regulation of ERK1 and ERK2 cascades, the chemokine-mediated

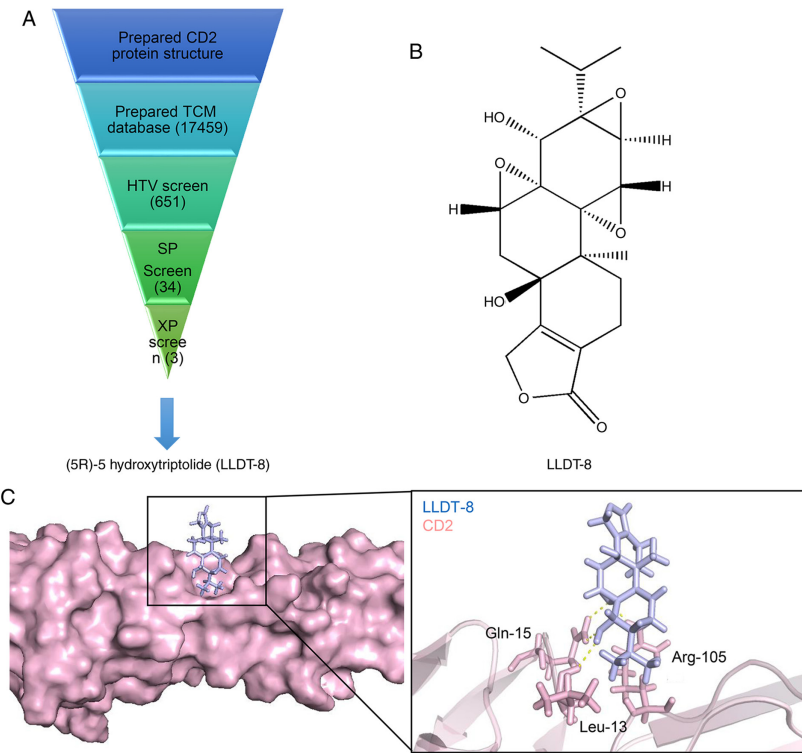


Figure 5. Binding mode of receptor-ligand interaction. (A) Flowchart of the CD2 inhibitor discovery strategy used in the present study. (B) 2D combination mode of CD2-LLDT-8. (C) Protein surface binding mode of CD2-LLDT-8. CD2, T-cell surface antigen CD2.

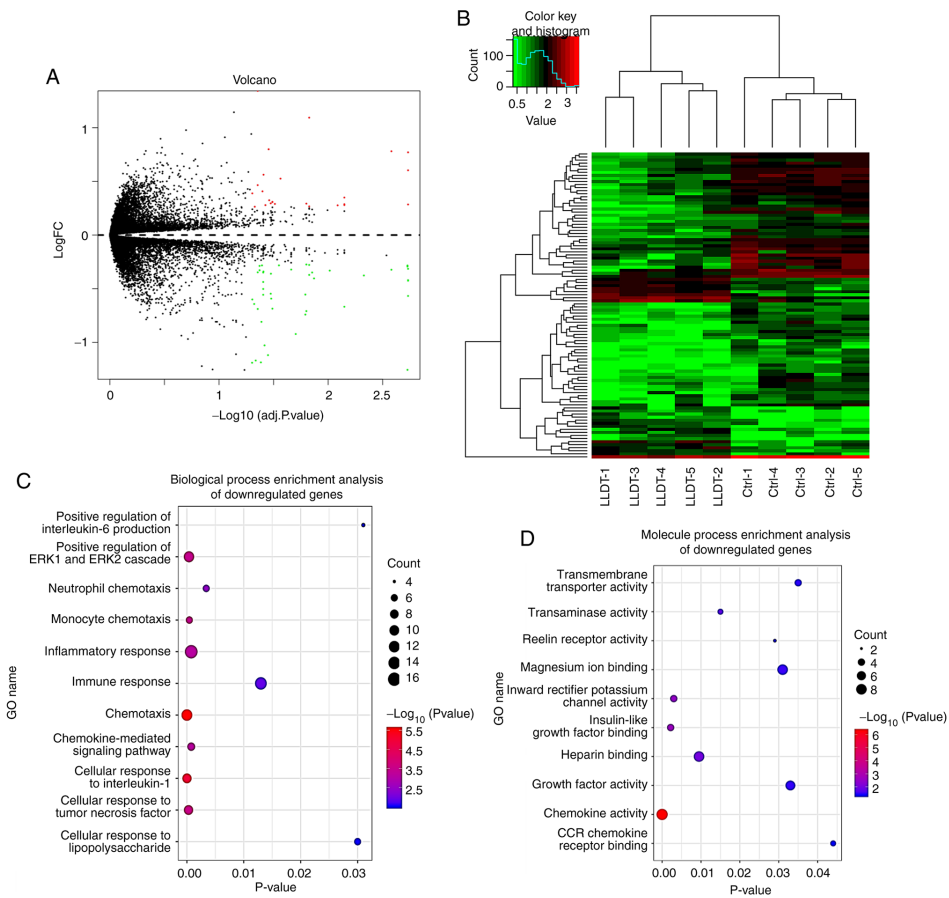


Figure 6. Identification of DEGs in RA tissues treated with LLDT-8. (A) Volcanic map of the differentially expressed genes between the LLDT-8-treated RA group and the RA control group. Red and green dots indicate the upregulated and downregulated genes, respectively. (B) Heatmap of DEGs between LLDT-8-treated and RA-controlled tissues based on the expression profiles. (C) Biological process and (D) Molecular function analyses of the downregulated genes in the LLDT-8 treated RA tissues. DEG, differentially expressed gene; RA, rheumatoid arthritis; FC, fold change; GO Gene Ontology.

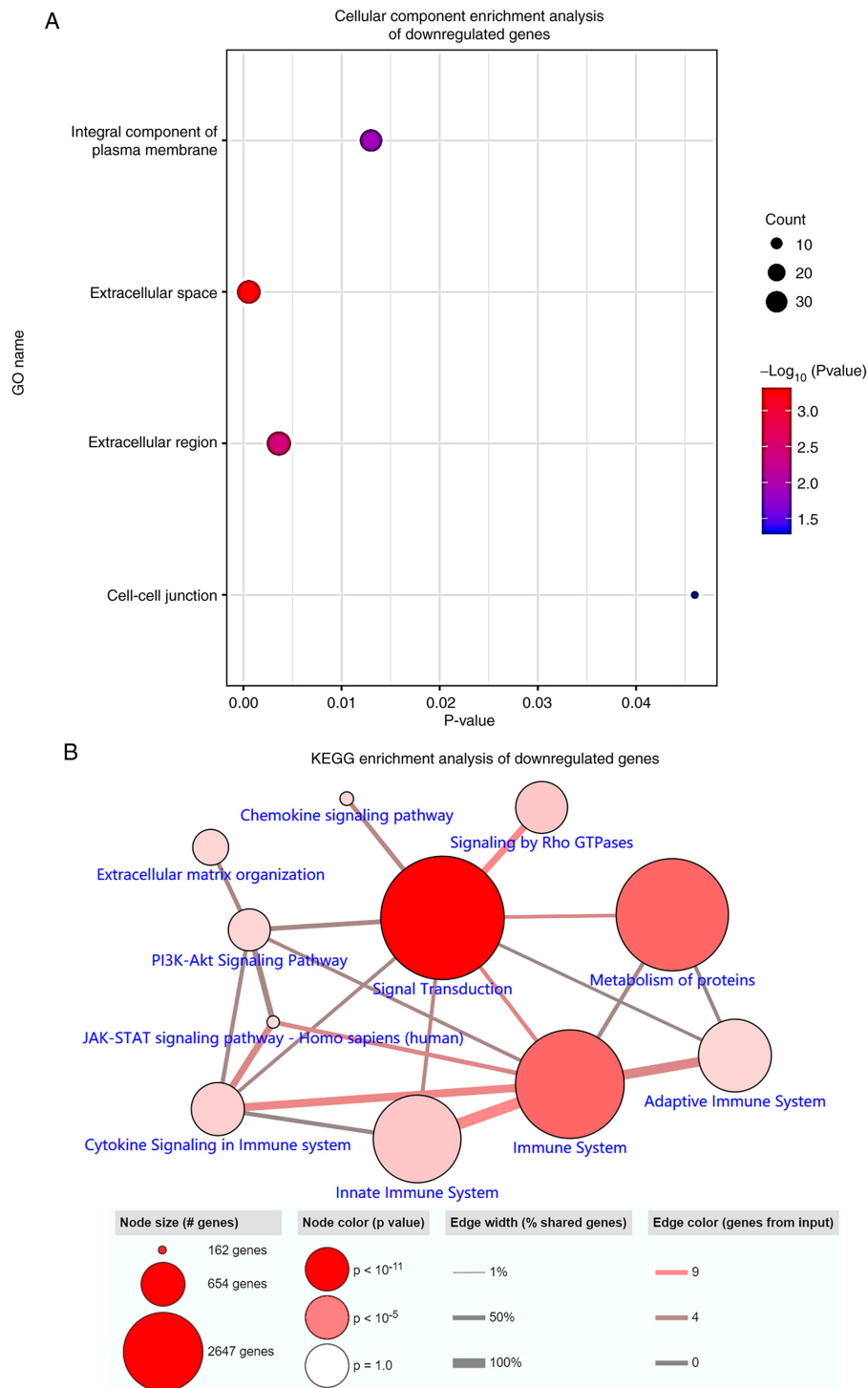


Figure 7. LLDT-8 widely suppresses immune-related functions and pathways. (A) Cellular component and (B) KEGG enrichment analyses of genes predicted to be downregulated by LLDT-8 in RA tissues. KEGG, Kyoto Encyclopedia of Genes and Genomes.

signaling pathway, inflammatory and immune responses, the positive regulation of IL-6 production function and chemokine signaling pathway, innate and adaptive immune systems, and the JAK-STAT signaling pathway in the RA process (Fig. 7B).

LLDT-8 treats RA by inhibiting CD2. Based on high-throughput molecular screening results, it was found that LLDT-8 inhibited CD2. Therefore, the changes in the levels of CD2 were detected in the LLDT-8 treated synovial cells. The experimental

results showed that compared with the control group, LLDT-8 reduced the expression of CD2 (Fig. 8A). The results of cell proliferation experiments showed that TNF- α could inhibit the proliferation of synovial cells, whereas LLDT-8 treatment restored the proliferation of synovial cells (Fig. 8B).

Further, changes in cellular inflammatory factors were detected. The experimental results showed that, compared with the control group, TNF- α stimulation increased the levels of inflammatory factors, whereas knockdown of CD2 reduced the stimulation of TNF- α . After knocking down CD2, the

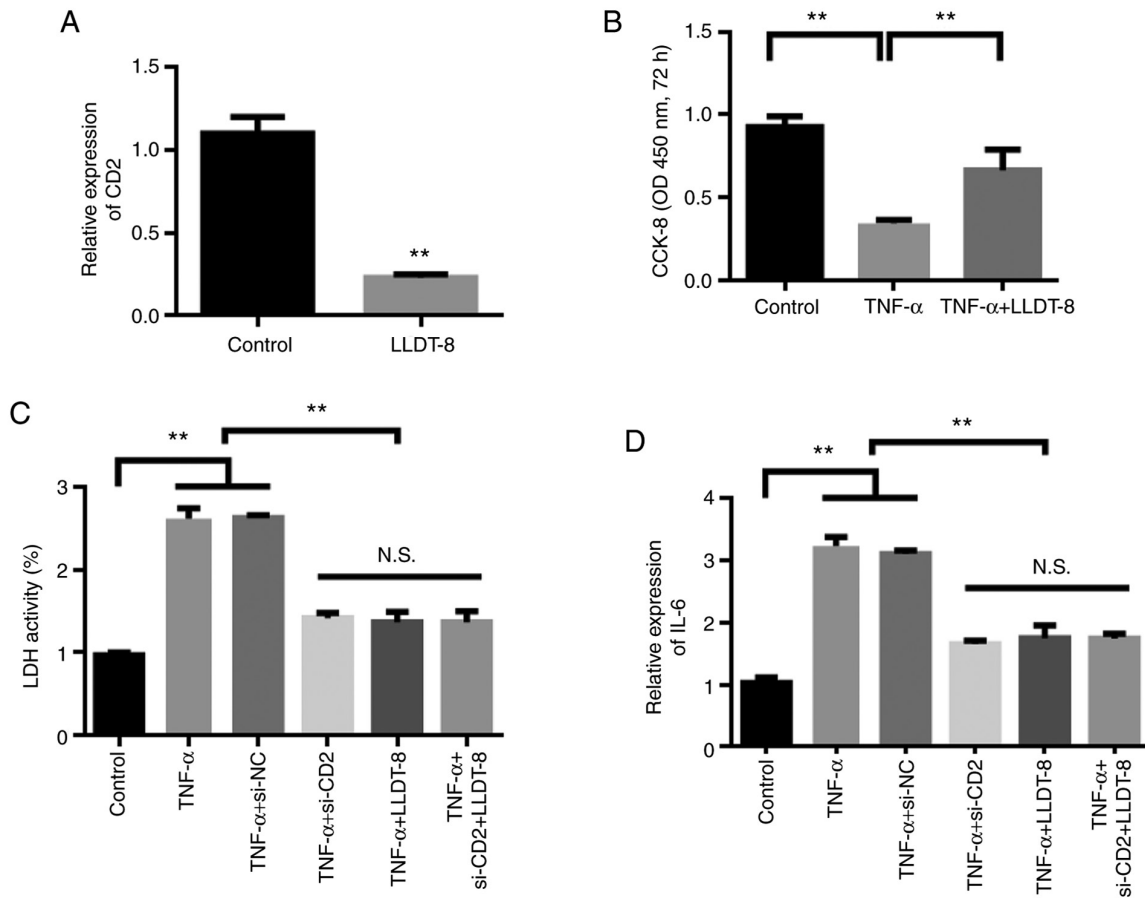


Figure 8. LLDT-8 exerts its beneficial effects on RA by inhibiting the expression of CD2. (A) LLDT-8 reduces the expression of CD2. (B) Cell proliferation ability detection following the different treatments. (C) Expression of the cell inflammatory factor LDH was detected following the different treatments. (D) Expression of the cytokine IL-6 was detected following the different treatments. RA, rheumatoid arthritis; CD2, T-cell surface antigen CD2; CCK-8, Cell Counting Kit-8; OD, optical density; si, small interfering; NC, negative control; N.S., not significant. ** $P < 0.01$.

administration of LLDT-8 did not further reduce the levels of inflammatory factors, suggesting that CD2 was the target of LLDT-8 (Fig. 8C and D).

Discussion

RA is a chronic systemic disease with an unclear etiology, although genetic and environmental factors may affect its pathogenesis (1). Several mechanisms regarding the immune disorders in RA have been proposed (34), but none can fully explain its exact pathogenesis. Therefore, screening key node genes that regulate immune disorders combined with drugs targeting these key genes may have important potential value for the clinical treatment of RA.

Key signaling pathways or node genes can be screened from the cluttered omics data through joint bioinformatics analysis, and this method is widely used to improve our understanding of the pathogenesis of various diseases, such as cancer and Alzheimer's disease (35,36). In the present study, the DEGs between normal and RA tissues, based on data obtained from GEO, were identified. Topological analysis revealed that CD2, a special marker protein distributed on the surface of T and NK cells (37), was a key node gene regulating immune disorders during the pathogenesis of RA. As a receptor, CD2 transmitted signals into the cells to activate T and NK cell activities (38,39). During the progression of RA, disordered

immune system function primarily manifests as the activation of T and NK cells. Thus, the CD2 protein may serve a key role in the immune disorder of RA, and CD2 may serve as a potential target for treating RA. Synovial cell level studies have shown that knockdown of CD2 can reduce the progression of RA.

Through molecular simulation docking, the potential drug LLDT-8 was screened to obtain the molecule with the optimal targeting activity of CD2. LLDT-8, one of the primary active ingredients in *Tripterygium wilfordii* plants (40), is an epoxy diterpene lactone compound. *Tripterygium wilfordii* has therapeutic value for the management of RA due to the presence of a triptolide; however, its pharmacological properties remain unclear (41). The present study further discussed the specific mechanism of *Tripterygium wilfordii*-related compounds with regard to their anti-inflammatory and analgesic properties. According to the omics data analysis, LLDT-8 effectively inhibited the immune- and inflammation-related signaling pathways, showing the potential therapeutic value of LLDT-8 in RA. *In vitro* functional and phenotypic experiments further explained the role of CD2 in RA progression and the potential therapeutic activity of LLDT-8.

The present study has some limitations. This study only verified the effect of LLDT-8 at the cellular level, and subsequent studies should also verify the efficacy of LLDT-8 *in vivo*. In addition, the downstream molecular mechanism of LLDT-8 targeting CD2 inhibition also needs to be further studied.

In conclusion, the results of the present study may improve our understanding of the developmental process of RA and highlight LLDT-8 as potential novel and effective drug for the treatment of RA.

Acknowledgements

Not applicable.

Funding

This study was supported by the Natural Science Foundation of Tianjin (grant no. 16ZXMJSY00220).

Availability of data and materials

The datasets used and/or analyzed during the present study are available from the corresponding author upon reasonable request.

Authors' contributions

YL conceived and designed the study. WQ and LY performed the bioinformatics analysis. YL and MW performed the in situ analysis. YL and LZ wrote the manuscript. All authors read and approved the final manuscript. YL and LZ confirm the authenticity of all the raw data.

Ethics approval and consent to participate

Not applicable.

Patient consent for publication

Not applicable.

Competing interests

The authors declare that they have no competing interests.

References

- Falconer J, Murphy AN, Young SP, Clark AR, Tiziani S, Guma M and Buckley CD: Review: Synovial Cell Metabolism and Chronic Inflammation in Rheumatoid Arthritis. *Arthritis Rheumatol* 70: 984-999, 2018.
- Firestein GS and McInnes IB: Immunopathogenesis of Rheumatoid Arthritis. *Immunity* 46: 183-196, 2017.
- Kim SY, Schneeweiss S, Liu J, Daniel GW, Chang CL, Garneau K and Solomon DH: Risk of osteoporotic fracture in a large population-based cohort of patients with rheumatoid arthritis. *Arthritis Res Ther* 12: R154, 2010.
- Källberg H, Ding B, Padyukov L, Bengtsson C, Rönnelid J, Klareskog L and Alfredsson L; EIRA Study Group: Smoking is a major preventable risk factor for rheumatoid arthritis: Estimations of risks after various exposures to cigarette smoke. *Ann Rheum Dis* 70: 508-511, 2011.
- Klareskog L, Gregersen PK and Huizinga TW: Prevention of autoimmune rheumatic disease: State of the art and future perspectives. *Ann Rheum Dis* 69: 2062-2066, 2010.
- Viatte S, Plant D, Bowes J, Lunt M, Eyre S, Barton A and Worthington J: Genetic markers of rheumatoid arthritis susceptibility in anti-citrullinated peptide antibody negative patients. *Ann Rheum Dis* 71: 1984-1990, 2012.
- Hogan DB: Did Osler suffer from 'paranoia antitherapeuticum baltimorensis'? A comparative content analysis of *The Principles and Practice of Medicine* and *Harrison's Principles of Internal Medicine*, 11th edition. *CMAJ* 161: 842-845, 1999.
- McInnes IB and Schett G: Pathogenetic insights from the treatment of rheumatoid arthritis. *Lancet* 389: 2328-2337, 2017.
- Reis-Filho JS and Pusztai L: Gene expression profiling in breast cancer: Classification, prognostication, and prediction. *Lancet* 378: 1812-1823, 2011.
- Tan L, Yu JT, Tan MS, Liu QY, Wang HF, Zhang W, Jiang T and Tan L: Genome-wide serum microRNA expression profiling identifies serum biomarkers for Alzheimer's disease. *J Alzheimers Dis* 40: 1017-1027, 2014.
- Shen Y, Jiang T, Wang R, He S, Guo M, Zuo J and He D: (5R)-5-Hydroxytryptolide (LLDT-8) inhibits osteoclastogenesis via RANKL/RANK/OPG signaling pathway. *BMC Complement Altern Med* 15: 77, 2015.
- Chen Y, Zhang L, Ni J, Wang X, Cheng J, Li Y, Zhen X, Cao T and Jia J: LLDT-8 protects against cerebral ischemia/reperfusion injury by suppressing post-stroke inflammation. *J Pharmacol Sci* 131: 131-137, 2016.
- Ren YX, Zhou R, Tang W, Wang WH, Li YC, Yang YF and Zuo JP: (5R)-5-hydroxytryptolide (LLDT-8) protects against bleomycin-induced lung fibrosis in mice. *Acta Pharmacol Sin* 28: 518-525, 2007.
- Xie ZC, Dang YW, Wei DM, Chen P, Tang RX, Huang Q, Liu JH and Luo DZ: Clinical significance and prospective molecular mechanism of MALAT1 in pancreatic cancer exploration: A comprehensive study based on the GeneChip, GEO, OncoPrint, and TCGA databases. *Oncotargets Ther* 10: 3991-4005, 2017.
- Woetzel D, Huber R, Kupfer P, Pohlner D, Pfaff M, Driesch D, Häupl T, Koczan D, Stiehl P, Guthke R, *et al*: Identification of rheumatoid arthritis and osteoarthritis patients by transcriptome-based rule set generation. *Arthritis Res Ther* 16: R84, 2014.
- Guo S, Liu J, Jiang T, Lee D, Wang R, Zhou X, Jin Y, Shen Y, Wang Y, Bai F, *et al*: (5R)-5-Hydroxytryptolide (LLDT-8) induces substantial epigenetic mediated immune response network changes in fibroblast-like synoviocytes from rheumatoid arthritis patients. *Sci Rep* 9: 11155, 2019.
- Ritchie ME, Phipson B, Wu D, Hu Y, Law CW, Shi W and Smyth GK: limma powers differential expression analyses for RNA-sequencing and microarray studies. *Nucleic Acids Res* 43: e47-e47, 2015.
- R Core Team: A Language and Environment for Statistical Computing. R Foundation for Statistical Computing, Vienna, 2013. Available from <https://www.R-project.org/>.
- Team R: RStudio: Integrated Development for R. RStudio, Inc., Boston, MA, 2015. Available from URL <http://www.rstudio.com>.
- Xi X, Liu N, Wang Q, Chu Y, Yin Z, Ding Y and Lu Y: ACT001, a novel PAI-1 inhibitor, exerts synergistic effects in combination with cisplatin by inhibiting PI3K/AKT pathway in glioma. *Cell Death Dis* 10: 757, 2019.
- Shannon P, Markiel A, Ozier O, Baliga NS, Wang JT, Ramage D, Amin N, Schwikowski B and Ideker T: Cytoscape: A software environment for integrated models of biomolecular interaction networks. *Genome Res* 13: 2498-2504, 2003.
- Xi X, Chu Y, Liu N, Wang Q, Yin Z, Lu Y and Chen Y: Joint bioinformatics analysis of underlying potential functions of hsa-let-7b-5p and core genes in human glioma. *J Transl Med* 17: 129, 2019.
- Zhong W, Sun B, Gao W, Qin Y, Zhang H, Huai L, Tang Y, Liang Y, He L, Zhang X, *et al*: Salvianolic acid A targeting the transgelin-actin complex to enhance vasoconstriction. *EBioMedicine* 37: 246-258, 2018.
- Zhong W, Yang W, Qin Y, Gu W, Xue Y, Tang Y, Xu H, Wang H, Zhang C, Wang C, *et al*: 6-Gingerol stabilized the p-VEGFR2/VE-cadherin/ β -catenin/actin complex promotes microvessel normalization and suppresses tumor progression. *J Exp Clin Cancer Res* 38: 285, 2019.
- Yu G, Wang LG, Han Y and He QY: clusterProfiler: An R package for comparing biological themes among gene clusters. *OMICS* 16: 284-287, 2012.
- Livak KJ and Schmittgen TD: Analysis of relative gene expression data using real-time quantitative PCR and the $2^{-\Delta\Delta CT}$ method. *Methods* 25: 402-408, 2001.
- Scardoni G, Pletterlini M and Laudanna C: Analyzing biological network parameters with CentiScaPe. *Bioinformatics* 25: 2857-2859, 2009.
- Bader GD and Hogue CW: An automated method for finding molecular complexes in large protein interaction networks. *BMC Bioinformatics* 4: 2, 2003.
- Szklarczyk D, Gable AL, Lyon D, Junge A, Wyder S, Huerta-Cepas J, Simonovic M, Doncheva NT, Morris JH, Bork P, *et al*: STRING v11: Protein-protein association networks with increased coverage, supporting functional discovery in genome-wide experimental datasets. *Nucleic Acids Res* 47: D607-D613, 2019.

30. Bodian DL, Jones EY, Harlos K, Stuart DI and Davis SJ: Crystal structure of the extracellular region of the human cell adhesion molecule CD2 at 2.5 Å resolution. *Structure* 2: 755-766, 1994.
31. Zhong W, Liu P, Zhang Q, Li D and Lin J: Structure-based QSAR, molecule design and bioassays of protease-activated receptor 1 inhibitors. *J Biomol Struct Dyn* 35: 2853-2867, 2017.
32. DeLano WL: Pymol: An open-source molecular graphics tool. *CCP4 Newsletter on protein crystallography* 40: 82-92, 2002.
33. Reimand J, Isserlin R, Voisin V, Kucera M, Tannus-Lopes C, Rostamianfar A, Wadi L, Meyer M, Wong J, Xu C, *et al*: Pathway enrichment analysis and visualization of omics data using g:Profiler, GSEA, Cytoscape and EnrichmentMap. *Nat Protoc* 14: 482-517, 2019.
34. Catrina AI, Joshua V, Klareskog L and Malmström V: Mechanisms involved in triggering rheumatoid arthritis. *Immunol Rev* 269: 162-174, 2016.
35. Glaab E, Baudot A, Krasnogor N and Valencia A: TopoGSA: Network topological gene set analysis. *Bioinformatics* 26: 1271-1272, 2010.
36. Bao R, Huang L, Andrade J, Tan W, Kibbe WA, Jiang H and Feng G: Review of current methods, applications, and data management for the bioinformatics analysis of whole exome sequencing. *Cancer Inform* 13 (Suppl 2): 67-82, 2014.
37. Yang JJ, Ye Y, Carroll A, Yang W and Lee HW: Structural biology of the cell adhesion protein CD2: Alternatively folded states and structure-function relation. *Curr Protein Pept Sci* 2: 1-17, 2001.
38. Watzl C and Long EO: Signal transduction during activation and inhibition of natural killer cells. *Curr Protoc Immunol* 11: 17, 2010.
39. James JR and Vale RD: Biophysical mechanism of T-cell receptor triggering in a reconstituted system. *Nature* 487: 64-69, 2012.
40. Wong KF, Yuan Y and Luk JM: *Tripterygium wilfordii* bioactive compounds as anticancer and anti-inflammatory agents. *Clin Exp Pharmacol Physiol* 39: 311-320, 2012.
41. Bao J and Dai SM: A Chinese herb *Tripterygium wilfordii* Hook F in the treatment of rheumatoid arthritis: Mechanism, efficacy, and safety. *Rheumatol Int* 31: 1123-1129, 2011.



This work is licensed under a Creative Commons Attribution-NonCommercial-NoDerivatives 4.0 International (CC BY-NC-ND 4.0) License.